ELECTRONIC SUPPLEMENTARY INFORMATION

Effective medium theory based modeling of the thermoelectric properties of composites: Comparison between predictions and experiments in the glass-crystal composite system $Si_{10}As_{15}Te_{75}$-$Bi_{0.4}Sb_{1.6}Te_3$

J-B. Vaney[1,2], A. Piarristeguy[2], V.Ohorodniichuck[1], O.Ferry[1], A.Pradel[2], E.Alleno[3],

J.Monnier[3], E.B.Lopes[4], A.P. Gonçalves[4], G.Delaizir[5], C.Candolfi[1], A.Dauscher[1], B.Lenoir[1]

[1]*Institut Jean Lamour (IJL), UMR 7198 CNRS-Université de Lorraine, France*

[2]*Institut Charles Gerhardt (ICG), UMR 5253 CNRS-Université Montpellier 2, France*

[3]*Institut de Chimie et des Matériaux de Paris Est (ICMPE), UMR 7182 CNRS, CMTR, Thiais, France*

[4]*IST/ITN Instituto Superior Técnico, Universidade Técnica de Lisboa, P-2686-953 Sacavém, Portugal*

[5]*SPCTS, Université de Limoges UMR CNRS 7315, France*

contact author : jean-baptiste.vaney@univ-lorraine.fr

Contents:

A- Evolution of the density of the composite according to the crystalline fraction

Figure A displays the evolution of the density and relative density of the composite series. Since the crystalline phase displays a larger density (6.8 g/cm^3) than the glassy phase (5.2 g/cm^3), the absolute density of the composite naturally increases with the crystalline phase fraction. Within a 1% uncertainty in the measurement of the density and the possibility of a certain amount of porosity in the composites, the increase can be divided in two steps. The first step is a linear increase of the density, maintaining the relative density at an almost 100% value. The relative density nonetheless decreases from 30% crystalline fraction, reflecting weaker capability of the crystalline phase to be shaped under these experimental conditions.

Figure A. Evolution of the density and relative density of the series of composites SiAsTe-BiSbTe.

B- Description of the theoretical basis of the effective medium theory (EMT) and its generalized version (GEMT).

The effective medium theory (EMT) consists in a set of approximations that allow calculating the macroscopic properties of an inhomogeneous medium, based solely on the properties of the phases constituting the medium. It was initially developed by Bruggeman between 1935 and 1937 to calculate the dielectric constants and polarizabilities of heterogeneous crystalline media [1]. The central approximation of this theory is to consider each particle of each phase immersed in a matrix displaying the effective properties of the macroscopic material. Thus, by choosing appropriate fluxes and potentials for continuity equations, it becomes possible to derive the Eq.(B-1) for a given property χ

$$\sum_i \varphi_i \frac{\chi_i - \chi_e}{\chi_i + \frac{1 - L_i}{L_i} \cdot \chi_e} = 0 \qquad \text{(B-1)}$$

where φ_i is the volume fraction of the phase i, χ_i and χ_e are the properties associated with the phase i and with the effective medium, respectively, and with L_i as the depolarization factor of the phase i. For spherical particles in dimension 3, the value of L_i can be precisely calculated and equals to 1/3 [2], yielding the better-known form of Eq.(B-1) where $(1-L_i)/L_i$ equals to 2. In 1952, Landauer derived a subsequent equation to calculate the electrical conductivity in multi-phasic metallic media [3], leading to further developments in the composites field. The previous year, Odelevskii had in fact already applied the same formalism to the thermal conductivity [4]. These equations have also been widely used in various scientific domains such as mechanics [5, 6] or optics [7-9]. Further details about this theory can be found in numerous references [2, 10-12].

For the electrical conductivity σ and the thermal conductivity λ, the EMT theory leads to the following formula in the presence of two phases [3, 4]

$$\varphi_1 \frac{\sigma_1 - \sigma_e}{\sigma_1 + 2.\sigma_e} + \varphi_2 \frac{\sigma_2 - \sigma_e}{\sigma_2 + 2.\sigma_e} = 0 \qquad \text{(B-2)}$$

$$\varphi_1 \frac{\lambda_1 - \lambda_e}{\lambda_1 + 2.\lambda_e} + \varphi_2 \frac{\lambda_2 - \lambda_e}{\lambda_2 + 2.\lambda_e} = 0 \qquad \text{(B-3)}$$

where φ_1 and φ_2 are the volume fractions of the phases 1 and 2, respectively. The subscripts 1, 2 and e correspond to the phase 1, 2 and the effective medium, respectively.

In the frame of the EMT, the percolation threshold is solely determined by the depolarization factors L_i of each phase [11], in contradiction with experiments where both the shape of the grains and their distribution play a major role [13]. McLachlan et al. unified the EMT and percolation theories under a phenomenological model, valid for a two-phases compound with a distribution of asymmetric grains. This equation was originally successfully applied to superconductors [12, 13]. The generalized EMT equation (the so-called GEMT equation) for a given property χ of a two-phases composite is expressed as

$$\varphi_1 \frac{\chi_1^{1/t} - \chi_e^{1/t}}{\chi_1^{1/t} + A.\chi_e^{1/t}} + \varphi_2 \frac{\chi_2^{1/t} - \chi_e^{1/t}}{\chi_2^{1/t} + A.\chi_e^{1/t}} = 0 \qquad \text{(B-4)}$$

where A is a constant that depends on the actual percolation threshold φ_c (of the phase 2 in the phase 1) through the equation A = $(1-\varphi_c)/\varphi_c$, and t is a constant representing the asymmetry of the microstructure (in terms of connection between the grains). Both

factors are directly linked to the depolarization factors L_i of each phase as in Eq.(B-1). Using a φ_c of 1/3 and a t factor set to 1, the EMT is then obtained in the case of spherical grains. The factor t can be directly calculated in simple cases such as monodisperse and isotropic oriented or non-oriented grains. However, these two new parameters are difficult to assess prior to the experiment in general and have to be considered as free parameters in the fitting procedure. This new formalism can be directly applied to the electrical and thermal conductivities, yielding the equations

$$\varphi_1 \frac{\sigma_1^{1/t} - \sigma_e^{1/t}}{\sigma_1^{1/t} + A.\sigma_e^{1/t}} + \varphi_2 \frac{\sigma_2^{1/t} - \sigma_e^{1/t}}{\sigma_2^{1/t} + A.\sigma_e^{1/t}} = 0 \qquad \text{(B-5)}$$

$$\varphi_1 \frac{\lambda_1^{1/t} - \lambda_e^{1/t}}{\lambda_1^{1/t} + A.\lambda_e^{1/t}} + \varphi_2 \frac{\lambda_2^{1/t} - \lambda_e^{1/t}}{\chi_2^{1/t} + A.\lambda_e^{1/t}} = 0 \qquad \text{(B-6)}$$

where all the constants are the same as described in Eqs. B-2, 3 and 4.

C- Discussion on the effect of varying the electrical resistivity ratio on the presence of a ZT maximum

Contrarily to the effect of Seebeck coefficient and thermal conductivity ratios on the maximum ZT in composites, the effect of the electrical resistivity ratio on the ZT_{max} seems to be shallow. On Figure C, the evolution of this ratio along many orders of magnitude (from 10^2 to 10^7) is presented, while keeping the Seebeck coefficients and thermal conductivities are kept at favorable values (respectively 10 and 0.1). It is depicted that no electrical resistivity ratio allows for an improved ZT_{max}. This may be due to the fact that ρ drops dramatically after the percolation threshold φ_p, leaving values of $\rho(\varphi>\varphi_p)$ almost unchanged whichever ρ_1 may be. The dotted curves, where the ZT_{max} seems to be increased, reflect situations when the ZT of the matrix phase (phase

1) is set to higher values than the ZT of the embedded phase (phase 2). In a situation where phase 2 is an efficient thermoelectric material such as Bi_2Te_3, it does not represent the properties of any existing materials and even breaks Wiedermann-Franz law.

Figure C. Evolution of ZT with the crystalline fraction of phase 2 embedded in a matrix (phase 1), with different ratios of the electrical resistivity. No significant impact is observed on the maximum ZT nor on its phase 2 fractions. Dotted curves represent the cases where the properties of phase 1 have no physical values (very low resistivity together with very low thermal conductivity –exceeding Wiedermann-Franz law- and very high thermopower).

D- Discussion on the outcomes of using the GEMT on the presence of a ZT maximum

Figure D presents different scenarios of the GEMT with t varying between 1 and 2 and φ_c between 10 and 33%. These results emphasize the possibility of maintaining at least an increase in ZT while using the more complex GEMT model.
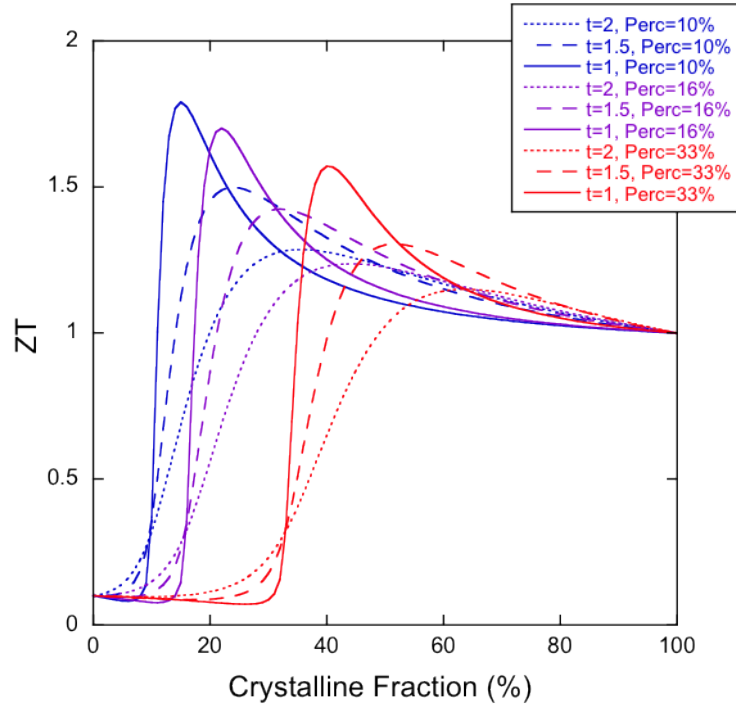
Figure D. Evolution of ZT as a function of crystalline fraction for different scenario with t varying between 1 and 2 and φc between 10 and 33%. In every case, an increase in the ZT values is predicted and is even more pronounced when the percolation crystalline fraction decreases.

When moving the percolation threshold from 33% to lower values, not only the maximum ZT is preserved but also increased. This feature can be explained by the combination of two factors. First, Seebeck coefficients and thermal conductivities are not strongly impacted by a shift in φ_p. For these two properties, it is due to a small contrast between the insulating and conducting materials properties to which we apply the EMT formalism (respectively λ/α and λ itself). On the other hand, for the electrical resistivity, the drop at φ_p is very sharp. With α and λ slightly favorable at lower crystalline fractions and the drop in ρ pushed back to lower values of φ, the resulting maximum ZT value is slightly enhanced.

As for the effect of t on the value of ZT_{max}, it reveals itself more difficult to be explained, due to the inherently elusive nature of t. This parameter embodies the asymmetry of the microstructure in favor of the embedded phase: when it increases, it

somehow translates the enhanced connectivity of this phase inside the matrix, at lower fractions, in a way, blurring out the percolation threshold. The maximum ZT would as well blur the electrical resistivity drop, pushing back ZT_{max} towards higher values of φ, together with slight decrease in magnitude as observed in Figure D.

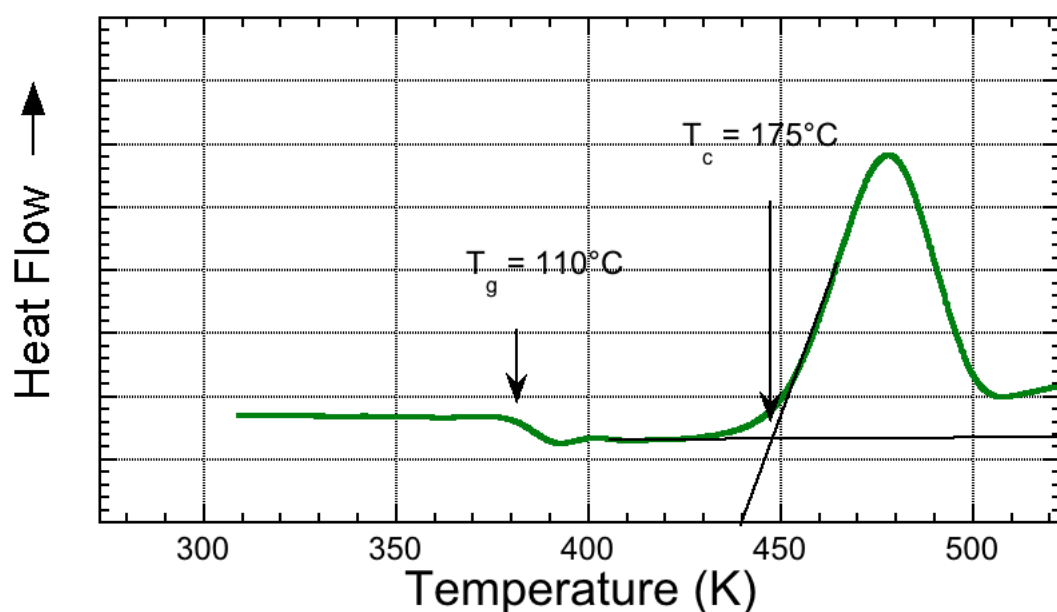## E- DSC study of the $Si_{10}As_{15}Te_{75}$ glassy phase

Figure E. DSC curve measured on the composition Si10As15Te75 with a 20K/min-heating rate.

F- Characterizations

Figure F-1. SEM (BSE) images at different scales of the surface of one composite sample with a crystalline fraction of 40%. The darkest phase is the glassy phase while the light grey one is the crystalline $Bi_{0.4}Sb_{1.6}Te_3$ phase.
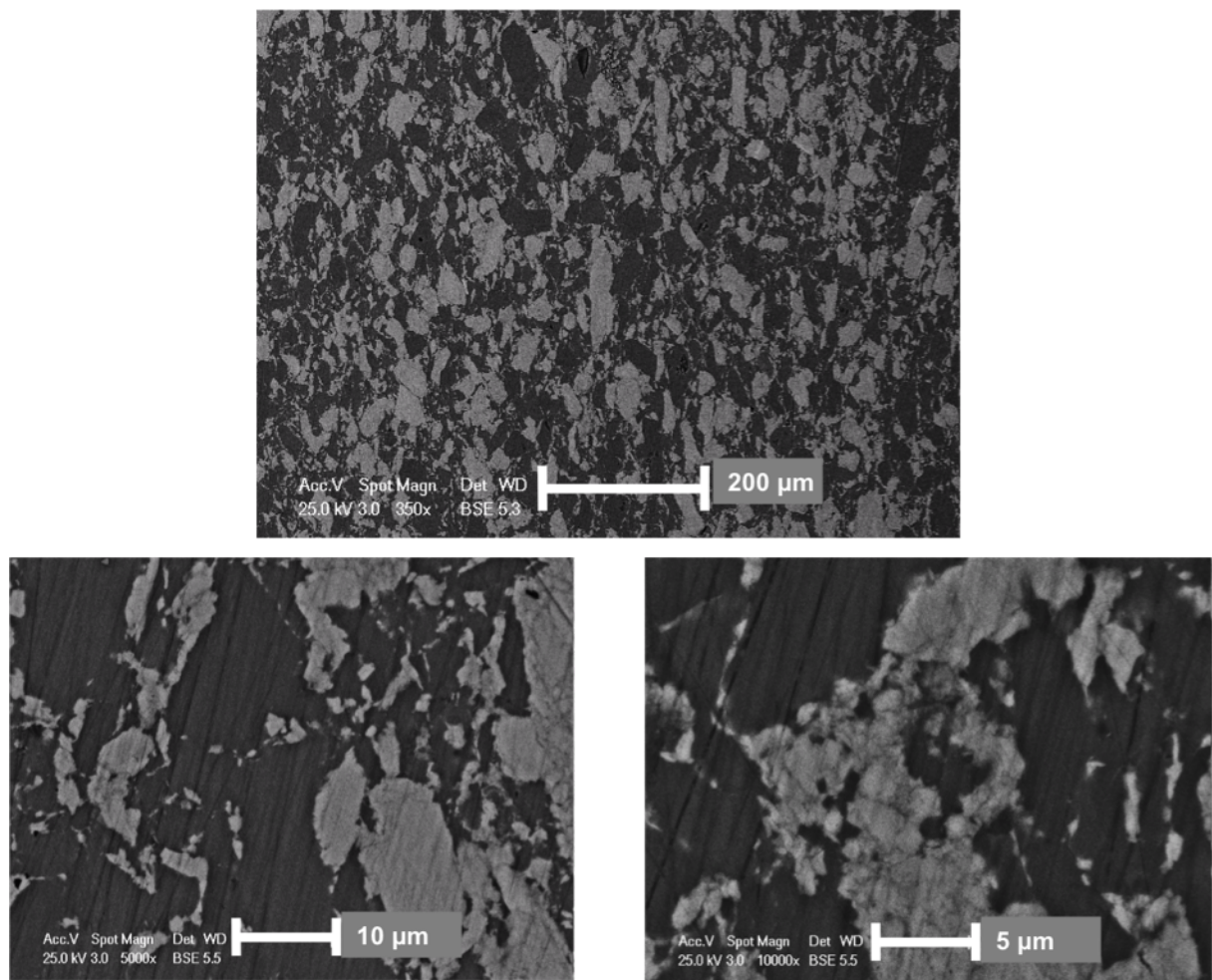
Figure F-2. EPMA performed on the 40% Bi0.4Sb1.6Te3 – 60% Si10As15Te75 composite. The left panel shows the line of measurements carried out while the right panel presents the chemical compositions obtained for each point probed in this region.
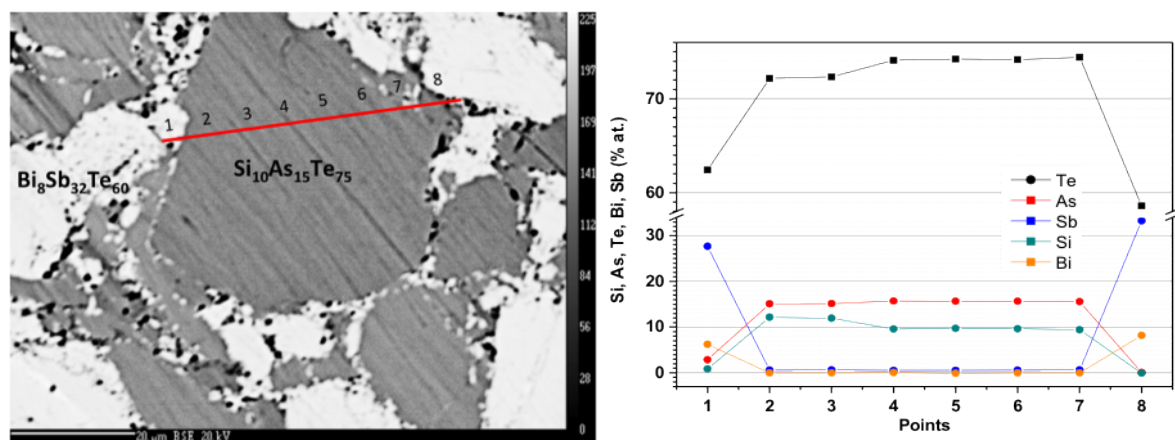
Figure F-2 displays the results obtained by EPMA, performed on the 40% $Bi_{0.4}Sb_{1.6}Te_3$ – 60% $Si_{10}As_{15}Te_{75}$ composite. The line measurement across a glassy region, including the two edging crystalline regions, allowed for probing composition of both phases. The averaged compositions of the glassy and crystalline phases were $Si_{11.1}As_{15.2}Te_{73.1}Sb_{0.56}$ and $Bi_{0.39}Sb_{1.71}Te_3$, respectively. These results seem to indicate Sb migration from the crystalline phase to the glassy phase. The same phenomenon was also observed for the 20-80 % composite.

Supporting materials references

1. D. Bruggeman, *Ann. Phys.*, 1936, **417**, 645-672.
2. R. Landauer, *AIP Conf. Proc.*, 1978, **40**, 2-45.
3. R. Landauer, *J. Appl. Phys.*, 1952, **23**, 779-784.
4. V. Odelevskii, *Zh. Tekh. Fiz*, 1951, **21**, 678-685.
5. A. Norris, *Mech. Mater.*, 1985, **4**, 1-16.
6. B. E. Hornby, L. M. Schwartz and J. A. Hudson, *Geophysics*, 1994, **59**, 1570-1583.
7. D. Wood and N. Ashcroft, *Philos. Mag.*, 1977, **35**, 269-280.
8. G. A. Niklasson, C. Granqvist and O. Hunderi, *Appl. Opt.*, 1981, **20**, 26-30.
9. F. Garcia-Vidal, J. Pitarke and J. Pendry, *Phys. Rev. Lett.*, 1997, **78**, 4289.
10. D. Stroud, *Phys. Rev. B*, 1975, **12**, 3368.
11. A. Davidson and M. Tinkham, *Phys. Rev. B*, 1976, **13**, 3261-3267.
12. D. S. McLachlan, *J. Phys. C Solid State*, 1987, **20**, 865.
13. D. S. McLachlan, M. Blaszkiewicz and R. E. Newnham, *J. Am. Ceram. Soc.*, 1990, **73**, 2187-2203.